

# Aerodynamic rotor loads prediction method with free wake for low speed descent flights<sup>1</sup>

B. Michéa<sup>2</sup>, A. Desopper, M. Costes

ONERA, Châtillon, France

## Abstract

A numerical method was developed to simulate a helicopter rotor at low speed and for descent flights. It consists of the coupling between a 3D unsteady full potential code, FP3D, and a new code derived from a lifting line method with vortex elements for the wake with prescribed geometry, METAR. This new code, MESIR, has a free wake analysis to get the capability to compute Blade-Vortex Interactions. Furthermore, the parts of the wake interacting with the blade are isolated and included in FP3D through a lifting surface approach. The method is validated with flight test results from the SA349 Gazelle helicopter and wind tunnel tests for the US Army OLS rotor in the DNW wind tunnel.

## 1 Introduction

Since the sixties and the seventies, the helicopter has emerged as a new efficient aircraft for civil applications thanks to its unique hover and vertical flight capabilities, which allow it to operate in difficult conditions, eg mountain rescue, off-shore oil rigs. Nevertheless, the use of helicopters for civil purposes did not increase as much as it could have. In particular they have been little used as a means of alleviating transport problems around major cities. One of the main reasons for this fact is the noise generated by the helicopter, and particularly, for an urban environment, low speed and descent flight Blade-Vortex Interaction noise (called BVI noise). This very impulsive noise is the result of periodic sudden aerodynamic disturbances induced by the wake which encounters the rotor blades, drastically modifying the local flow conditions. Consequently, one of the major issues for rotorcraft research is to reduce the noise generated by the helicopter to enlarge its use on the civil market. Noise reduction is also a big concern for military applications to decrease the aircraft detectability.

---

1 This work was supported by the French Ministry of Defence (STPA)

2 Thesis student, Université Pierre et Marie Curie (Paris VI)



The work described in this paper aims at computing the aerodynamic phenomena which occur during BVI. This step is necessary in view of predicting the noise generated by the rotor since any acoustic analysis needs the time dependent pressure distribution on the blade to propagate these perturbations in the far-field. In the case of highly impulsive noise, like BVI, the aerodynamic analysis has to be very accurate because the noise is mainly sensitive to pressure gradients. In order to simulate these phenomena precisely, a free-wake lifting line rotor analysis, called MESIR, was developed and coupled with a three-dimensional CFD code, FP3D, which solves the unsteady full potential equation. During the coupling process, the parts of the wake which interact with the blade are isolated, and the velocity field they induce on the blade is taken into account with a lifting surface approach, contrary to the rest of the wake which is taken into account with a simpler angle of attack approach. The new method is validated with flight test results obtained with a SA349 Gazelle flying at low speed with a pressure instrumented rotor, and with wind tunnel tests on the US Army OLS rotor for low speed descent flight conditions.

## 2 Calculation method

### 2.1 Introduction

Typical three-dimensional rotor calculations are performed with a three-dimensional unsteady full potential code, called FP3D [1]. This code solves the mass-conservation equation and the Bernoulli equation in a generalized coordinates system linked to the blade. The equation is solved around an isolated blade, and the space surrounding it is discretized in a grid box, covering generally six reference chords length around the blade and going spanwise from mid radius to one and a half rotor radii. The mass conservation equation is discretized using first order finite differences in time and second order centered finite differences in space. A first order density and flux terms linearization versus the velocity potential is applied to obtain an algebraic equation with the potential as single unknown. The implicit operator is approximately factored into three one-dimensional tridiagonal operators, one for each grid direction, which are easy to solve. The density, velocity and metric flux terms are computed at half points, with the same differencing scheme applied to the metric tensor as for the potential, which gives a consistent formulation in 2D, but a freestream correction term has to be subtracted from the discretized flux in 3D. For supersonic flows, a parameter-free Engquist-Osher flux biasing scheme [2] is applied to upwind the density in the flux terms, allowing to simulate correctly the domain of dependance at the grid points. The boundary conditions are a transpiration condition on the blade surface, 2D perturbation flow for the inner section and nonreflecting boundary conditions at the grid boundaries. For a lifting rotor, the wake shed from the trailing edge, which appears in the calculation as a potential jump, has to be convected downstream. The transport equation is obtained from the Bernoulli equation assuming that the pressure is continuous across the wake. Furthermore, in the case of a lifting rotor, an external rotor model is necessary since the full potential equation is solved around an isolated blade. The model used is METAR [3], from Eurocopter France.

The METAR code simulates the rotor with a lifting line following the quarter chord line of each blade, and the wake is discretized with vortex elements with prescribed

geometry. Generally, a helicoidal shape is used for the wake. The blade sections are simulated through the polars of the airfoils defining the blade geometry. The code needs the blade motion, pitch and flap, as input, and iterates on the circulation distribution on the blade and in the wake until convergence. The wake induced velocities at the quarter chord line are computed with the Biot and Savart law.

The METAR influence into the FP3D calculation is introduced with an angle of attack approach. The part of the wake which is not taken into account in the FP3D calculation (ie the whole wake except the part of it shed from the discretized blade, connected to it and included in the grid box), is used to compute, with the Biot and Savart law, the far wake induced velocity for each grid spanwise station and for a discrete number of azimuthes. A Fourier decomposition allows interpolation in time and therefore the definition of the local angle of attack for each time step of the FP3D calculation. This space and time dependent angle of attack is imposed in the FP3D boundary conditions through a constant chordwise transpiration angle at the blade surface.

Good correlation with experiment was found with such an approach with wind tunnel or flight tests results for a rotor in high-speed forward flight [4]. However, this analysis is not adapted to compute low speed and descent flight. The first reason for that, is that the wake geometry has a very large influence on the pressure distribution for these flight conditions, and a prescribed wake geometry, unless especially tuned for the case considered, cannot simulate the true flow conditions satisfactorily. Furthermore, a vortex interacting closely with the blade induces steep local pressure gradients which cannot be correctly simulated with an angle of attack approach in FP3D [5]. Consequently, a free wake version of METAR was developed to compute the wake geometry correctly at low speed and descent conditions, and a new coupling approach between FP3D and MESIR, the free wake version of METAR, taking into account the vortex motion around the blade through a chordwise dependent induced velocity, was adopted. This method is similar to the one developed by Hassan et al. [6].

## 2.2 MESIR code

The MESIR code is a development of METAR, in which a time marching free wake analysis was included. In the initial METAR formulation, the vortices are convected using a uniform induced velocity given by the Meijer-Drees formula. Therefore the vortex trajectories are straight lines. The free wake approach consists of computing the local velocities induced by the wake on each point representing the vortex lattice, and in convecting the vortices with these velocities. These vortex velocities are given by the Biot and Savart law. This azimuth-marching procedure can then be summarized as follows :

- consider a vortex of age  $j$ , located at point  $\vec{X}_j$  when the blade is at the azimuth  $\psi_j$ , and the velocity,  $\vec{V}_j$ , induced on this vortex by the whole wake and the blades, computed by the Biot and Savart law.
- the new vortex position  $\vec{X}_{j+1}$  at the azimuth  $\psi_{j+1}$  ( $\psi_{j+1} = \psi_j + \Delta\psi$ ) is given by the formula:  $\vec{X}_{j+1} = \vec{X}_j + \vec{V}_j \cdot \Delta t$ . The age of the vortex is now  $j+1$  and the

time-increment  $\Delta t$  corresponds to the elementary rotation  $\Delta\psi$ , the value of which is  $15^\circ$  in the calculations shown in this paper.

Three rotor rotations are computed for the wake, and they are divided into two regions: a near wake, which represents the two first rotor rotations, and a far wake, which represents the third wake rotation included in the calculation. The near wake vortices are computed using the free wake process described above, while the far wake vortices are convected using the classical Meijer-Drees velocities, as is done in METAR for the whole wake. The free wake analysis is started when the blade is at the azimuth  $\psi=0^\circ$  from a METAR calculation (ie with a wake geometry and a circulation distribution computed by METAR) and marches step by step until the blade has completed three rotations. At this time, a new circulation distribution has to be computed to be consistent with the new wake geometry. This process is iterated until convergence is obtained on the wake geometry. Typically, three iterations are necessary at low speed to reach a satisfactory level of convergence.

### 2.3 The coupled method (MESIR-FP3D)

In order to study the BVI characteristics and to compute the BVI perturbations accurately the MESIR and FP3D codes were modified. A special subroutine was developed in MESIR for this objective. This subroutine computes the BVI locations on the rotor disk and the most important interaction parameters: the distance and the angle between the vortex and the blade, and the vortex circulation. Then a "BVI wake" is built, including the part of the tip vortex which interacts with the blade, for each interaction which was detected. The velocities induced by this region of the wake are computed at every point of the blade grid in FP3D, while the influence of the remaining part of the wake is only computed at the quarter chord line. The BVI wake is taken into account before and after the interaction, to avoid unphysical disturbances on the calculated velocities. It is also interpolated in time, to compute the perturbations more accurately than with the time step presently used in MESIR ( $15^\circ$ ). The new time step used for this part of the wake is equal to  $2^\circ$ . This process allows the major part of the perturbation levels to be taken into account. Finally, the contribution of all the interactions are added to compute the local induced velocities at each point on the blade. They are taken into account in the FP3D boundary conditions through a transpiration angle variable in chord, span and azimuth, using a Fourier decomposition.

## 3 Results and discussion

### 3.1 Gazelle flight test

The method was first applied to the Gazelle helicopter, for which flight test results at low speed forward flight ( $\mu=0.146$ ) with an instrumented rotor are available [7]. In this case, contrary to descent flight, blade-vortex interactions are weak, but the local loads are very sensitive to the wake geometry. The computed free wake shows good agreement with

theoretical knowledge and with experimental visualizations [8]. The tip vortices move up in the regions of the advancing and the retreating blade ( $\psi=90^\circ$  and  $270^\circ$ ) and their roll-up is well simulated (Figure 1). Because of the big strength of the tip vortices, the inner sheet is also moved down. This is in good agreement with the well-known analogy with the flow behaviour downstream a fixed wing (Figures 2 and 3).

The free wake analysis has very little influence on the BVI locations (Figure 4), but the distance between the blade and the vortices during the interaction is greatly modified. While, for the prescribed geometry, the nearest vortices are located 0.6 chord below the blade, most of the vortices, in the free wake calculations, remain very close to the blade, from 0.6 chord beneath to 0.2 chord above the blade (Figure 5). Consequently, bigger perturbations on the blade loads are induced by the free wake approach. This is in good agreement with experiment, where the lift gradients around  $90^\circ$  and  $270^\circ$  are well estimated by MESIR (Figure 6), while METAR clearly underestimates them. This is due to the close passage of the BVI wake to the blade, inducing then strong variations in the local inflow. Similar calculations, using FP3D, show the same tendency (Figure 7). Nevertheless, the azimuthal lift evolution is smoother than with MESIR or METAR alone, and very good correlation with experiment is found. For these calculations, the same approach was chosen to include the wake influence from MESIR and METAR (induced velocities computed at the quarter chord line only). Considering that no strong BVI occurs for this test case, a lifting surface approach was not performed.

Figure 8 shows the lift evolution versus the azimuth for two sections (88 and 97 %). The MESIR + FP3D results are compared to experiment and a good agreement is found. The load evolutions are particularly well predicted at BVI locations, in phase and intensity. Good correlation for the chordwise pressure distribution is also found (Figure 9).

### 3.2 OLS wind-tunnel test

The method was also applied to the U.S. Army O.L.S. rotor, for which wind-tunnel test results at low speed descent flight ( $\mu=0.146$ ,  $\alpha_q=1.5^\circ$ ) are available [9]. These results were obtained in the D.N.W. wind-tunnel. One blade section (0.955 R) was instrumented with unsteady pressure transducers and the blade leading edge (0.03 c) had several differential pressure transducers distributed along the span. In this case, Blade-Vortex Interactions can be very strong and blade-vortex encounters may happen. The free wake calculation (Figures 10 and 11) confirms that close BVIs occur on the advancing and on the retreating blade side. Therefore the vortex core value was decreased, because its usual value (0.5 chord) removed most of the interactions from the calculation. A new 0.2 chord vortex core value was then selected. Furthermore, the chordwise velocity distribution due to BVI was included in MESIR + FP3D calculation ("Lifting Surface" approach).

Figure 12 shows the differential pressure evolution versus the azimuth, at  $x/c=0.03$  and for four blade sections. The pressure fluctuations due to BVI are clearly noticeable for all the sections, and reasonably well predicted by the method. The perturbations level is underestimated for the retreating blade, but well calculated on the advancing blade side. Very good correlation can be observed for the phases, showing that the BVI locations are well predicted. Figure 13 shows the differential pressure evolution versus the azimuth, at  $r/R=0.955$  and for two chordwise positions. The perturbation levels and gradients are well

estimated at  $\psi=280^\circ$ , but overestimated at  $\psi=300^\circ$ . Fairly good correlation can be observed for the BVIs from  $\psi=60^\circ$  to  $\psi=90^\circ$ , even if small fluctuations are removed from the calculation. A finer wake discretization could improve the results. Good correlation for the chordwise pressure distribution is also found at this station (Figure 14), except at  $\psi=45^\circ$  where the pressure level is overestimated. In particular, the shock position and strength are very well estimated at  $\psi=90^\circ$ .

## 4 Conclusions

A new version of the METAR code, called MESIR, was developed to compute BVI accurately. For that purpose, a free wake analysis, a special representation for the "BVI wake" and a Lifting Surface approach were included to give the inflow to the Full Potential FP3D code. This new code is able to perform BVI calculations with improved correlation with experiment. In particular, the free wake geometry shows good agreement with theory and experimental visualization. The improved calculation of the BVI wake, with a finer discretization, allows to take into account the BVI perturbations correctly on the blade. Finally, the Lifting Surface approach to compute the boundary conditions in FP3D improves the results of the method in the case of very strong interactions. Further improvements can be introduced, in particular in reducing the time step in MESIR and also in refining the coupling between MESIR and FP3D, in order to simulate close encounters between the wake and the blade.

## References

- [1] Costes M. *Présentation d'une méthode de calcul potentiel complet des vitesses pour rotors d'hélicoptère*. R.T. ONERA n° 151/1369AY. Oct. 1987.
- [2] Hirsch C. *Numerical computation of internal and external flows. Vol. 1 Computational methods for inviscid and viscous flows*. John Wiley & Sons. 1988.
- [3] Toulmay F. *Modèle d'étude de l'aérodynamique du rotor*. Rapport Eurocopter-France n° R 371.76. 1986.
- [4] Costes M., Desopper A., Ceroni P. & Lafon P. *Flow field prediction for helicopter rotor with advanced blade tip shape using CFD techniques*. Presented at the 2<sup>nd</sup> Int. Conf. on Basic Rotorcraft Research. College Park (University of Maryland), feb. 1988.
- [5] Jones H.E. & Caradonna F.X. *Full potential modeling of blade-vortex interactions*. NASA technical memorandum 88355. Aug. 1986.
- [6] Hassan A. A., Tung C. & Sankar L. N. *An assesment of full potential and Euler solutions for self-generated rotor blade-vortex interactions*. Presented at the 46<sup>th</sup> Annual Forum of the American Helicopter Society. Washington, may 1990.
- [7] Yamauchi G. K., Hefferman R. M. & Gaubert M. *Correlation of SA 349/2 helicopter flight test data with a comprehensive rotorcraft model*. Presented at the 12<sup>th</sup> European Rotorcraft Forum. Garmisch-Partenkirchen, sept. 1986.
- [8] Egolf T. A. & Landgrebe A. J. *Generalized wake geometry for a helicopter in forward flight and effect of wake deformation on airloads*. Presented at the 40<sup>th</sup> Annual Forum of the American Helicopter Society. Crystal City, may 1984.
- [9] Boxwell D. A., Schmitz F. S., Spletstoeser W. R. & Schultz K. J. *Model helicopter rotor high speed impulsive noise: measured acoustic and blade pressures*. Presented at the 9<sup>th</sup> European Rotorcraft Forum. Stresa, sept. 1983.

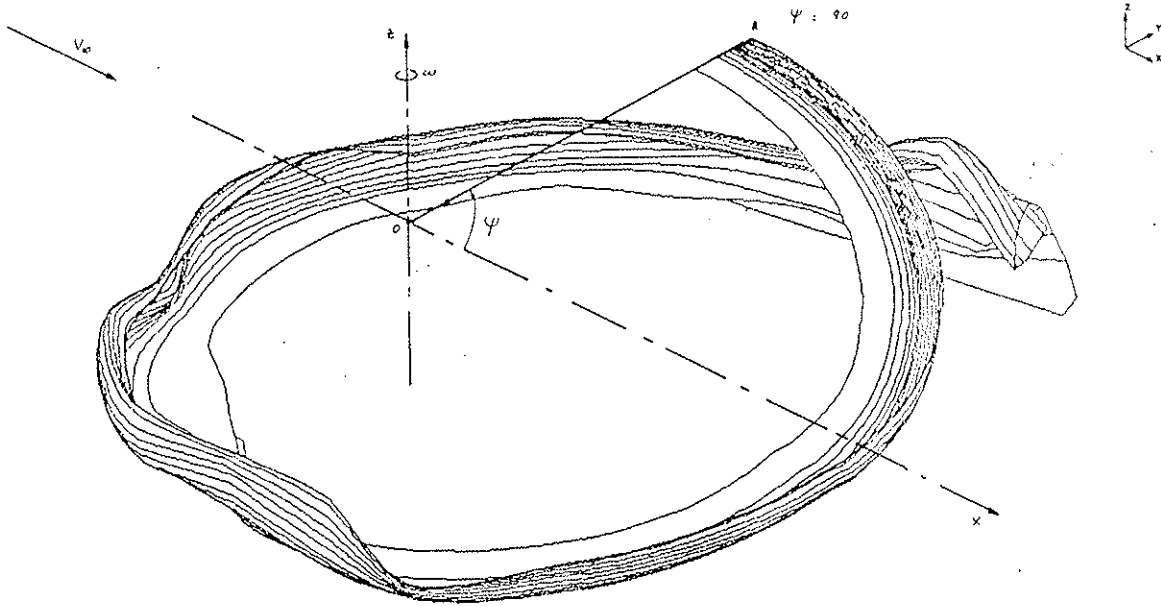


Fig. 1 - First turn of rotor (blade at  $90^\circ$ ).

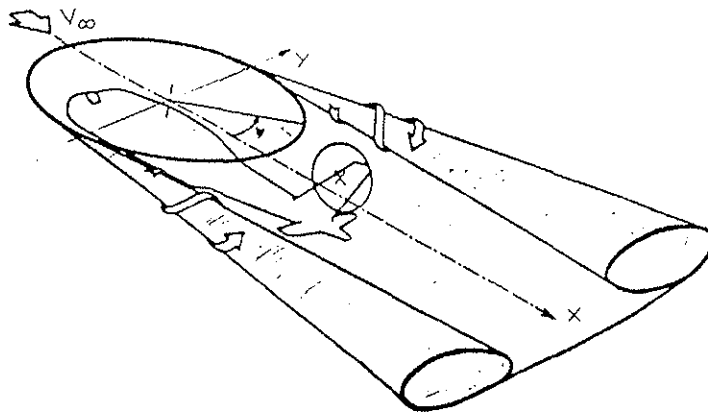


Fig. 2 - Fixed wing analogy.

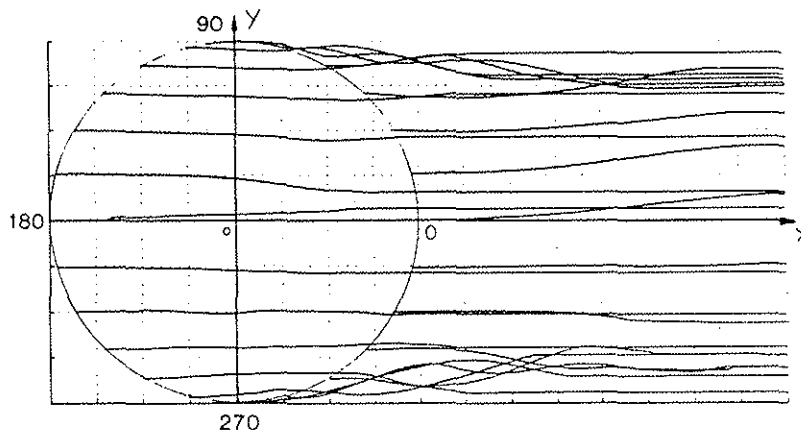


Fig. 3 - Tip vortex trajectories.



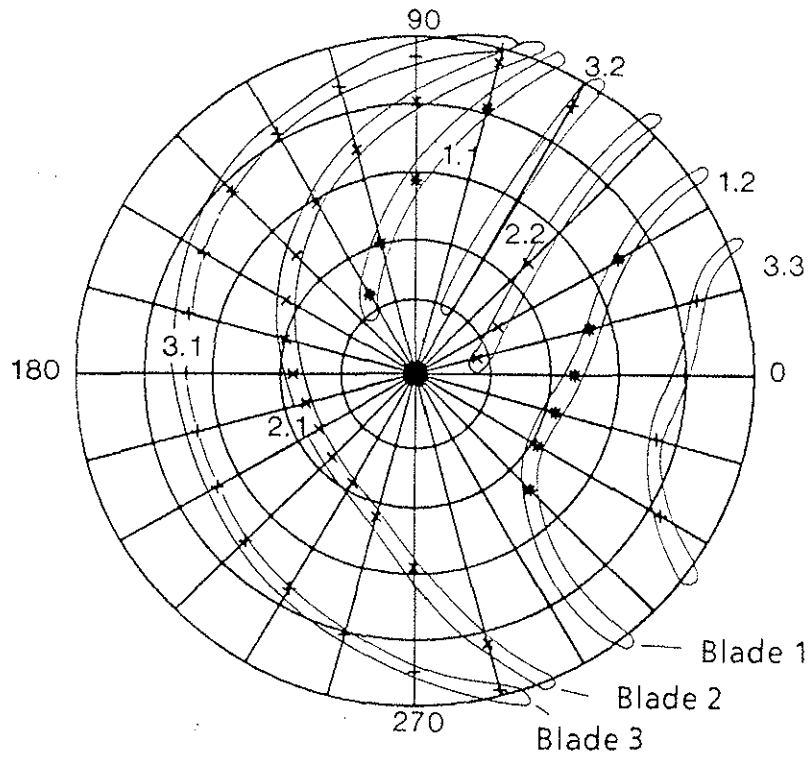


Fig. 4 - Blade vortex interactions location on the rotor disk.

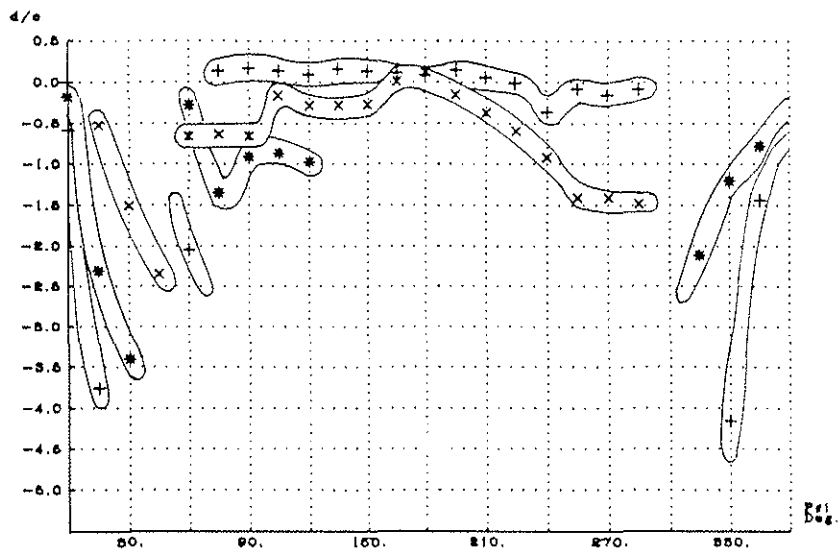


Fig. 5 - Vertical distance between the vortex and the blade.

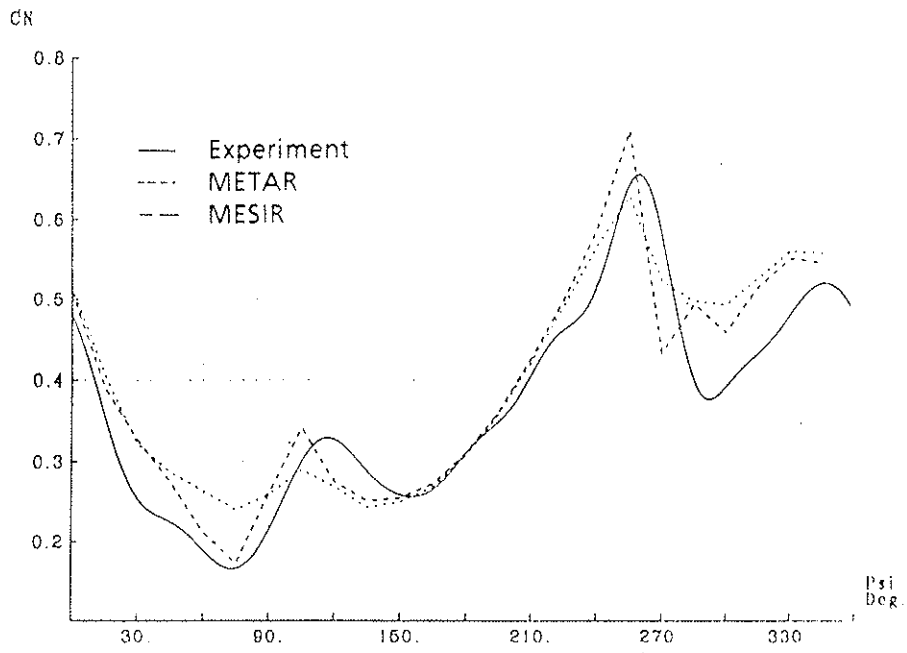


Fig. 6 - Gazelle flight test, local loads at  $r/R = 0.88$ .

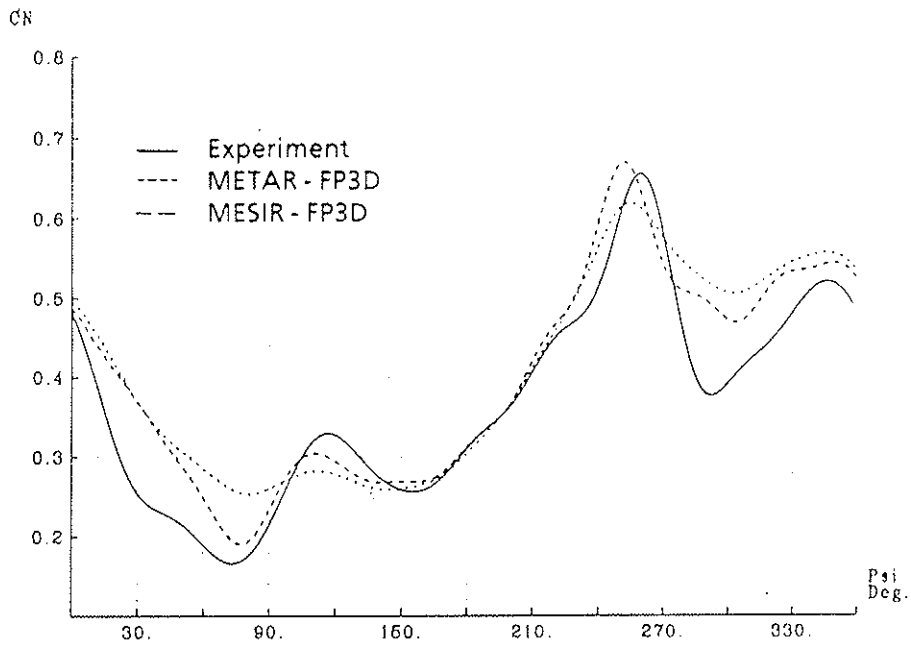


Fig. 7 - Gazelle flight test, local loads at  $r/R = 0.88$ .

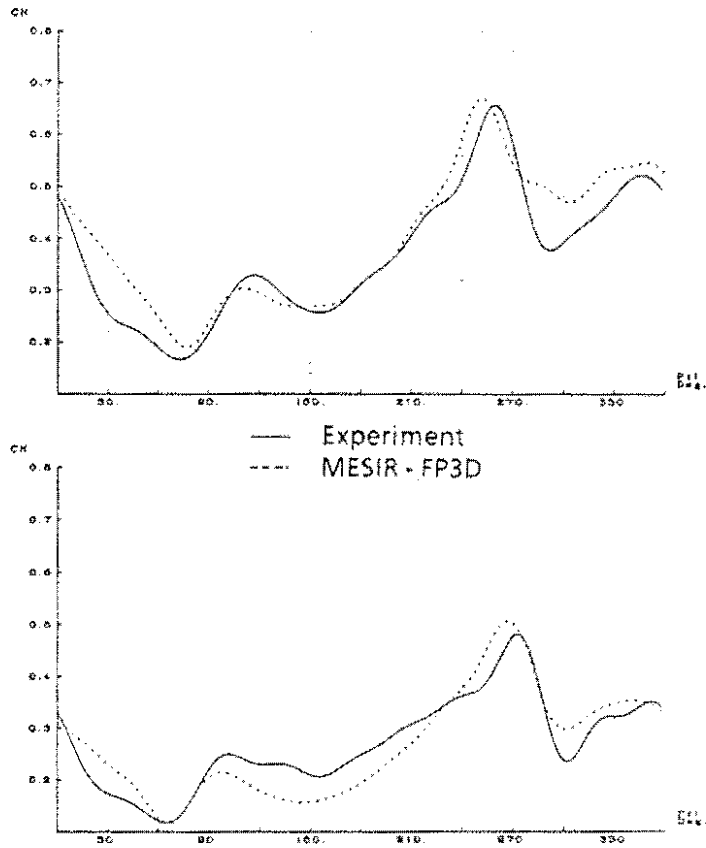


Fig. 8 - Gazelle flight test, local loads at  $r/R = 0.88$  and  $0.97$ .

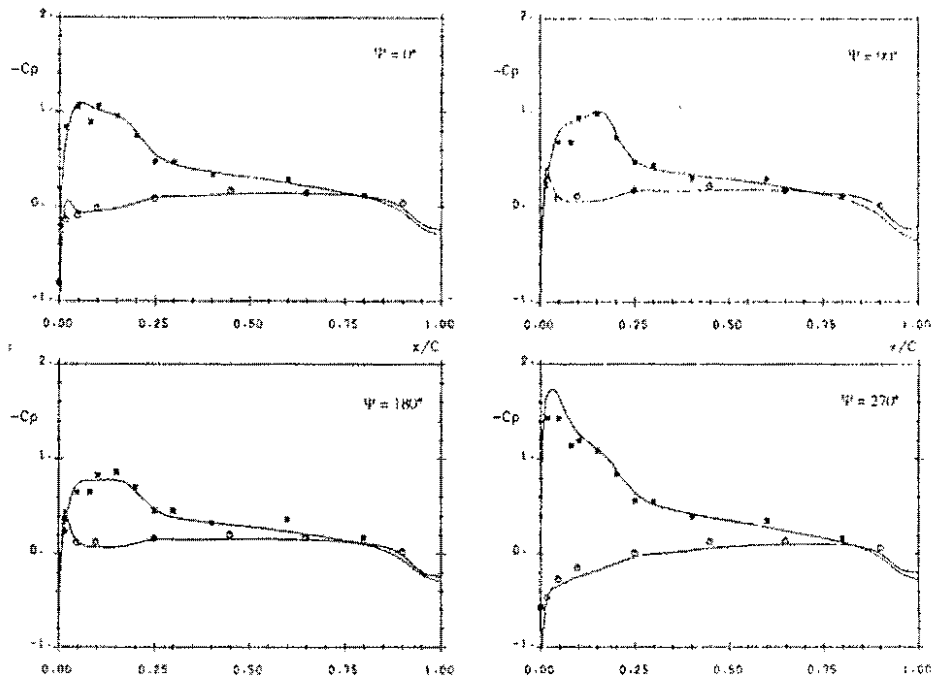


Fig. 9 - Gazelle flight test, chord wise pressure distribution at  $r/R = 0.97$ .

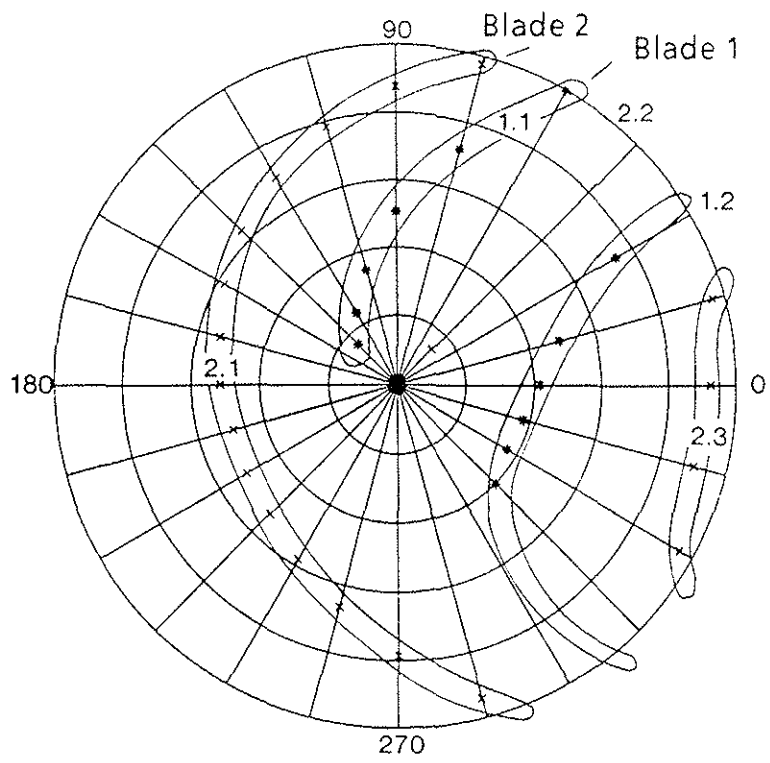


Fig. 10 - BVI location on the rotor disk.

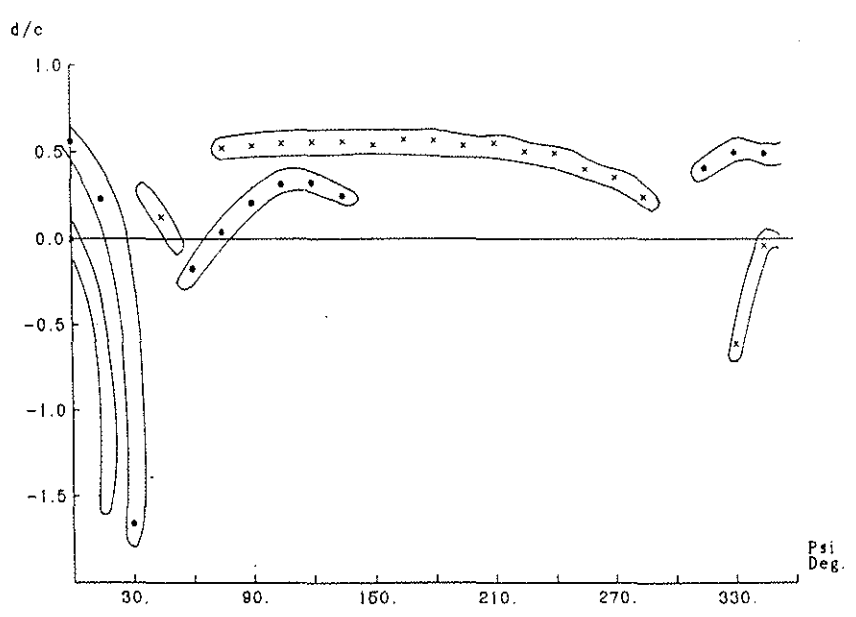


Fig. 11 - Vertical distance between the vortex and the blade.

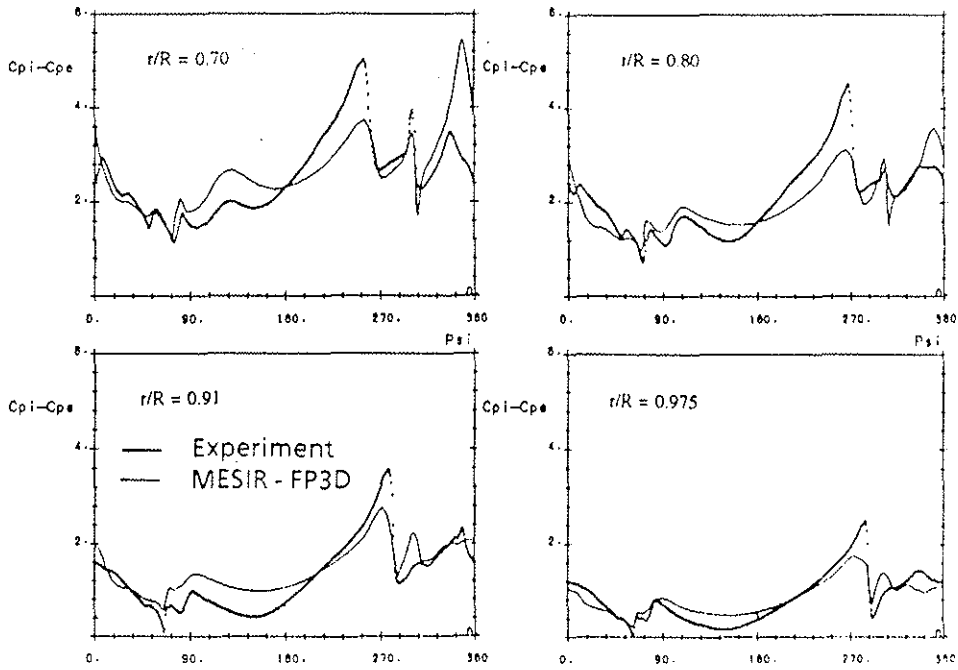


Fig. 12 - Differential pressure at  $x/c = 0.03$ .

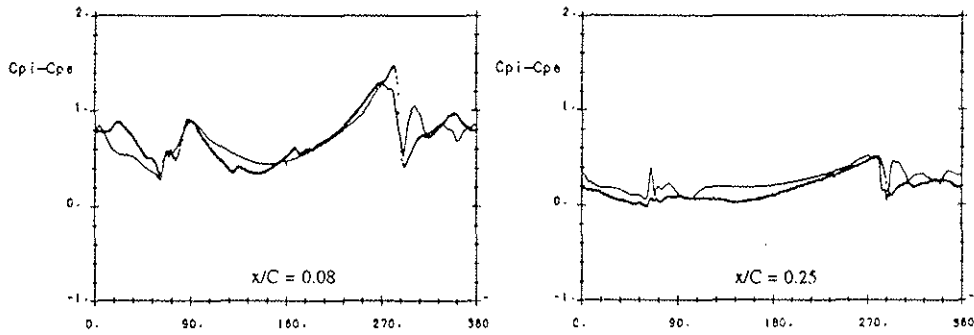


Fig. 13 - Differential pressure at  $r/R = 0.955$ .

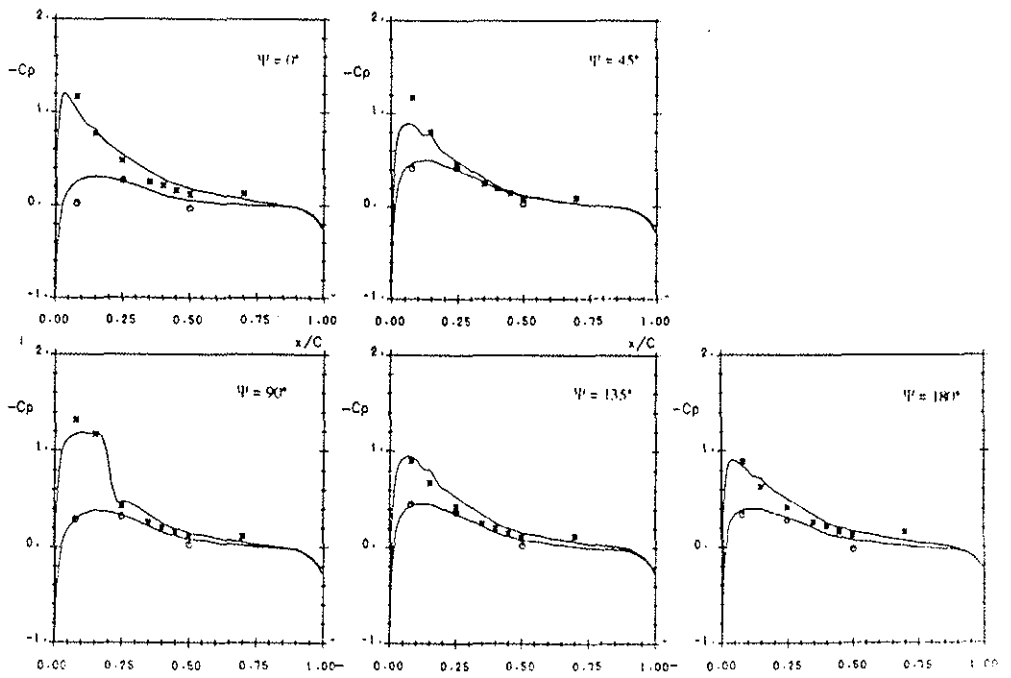


Fig. 14 - Chordwise pressure distribution at  $r/R = 0.955$ .